

# Nonlinear parametric model for Granger causality of time series

Daniele Marinazzo<sup>1,2,3</sup>, Mario Pellicoro<sup>1,2,3</sup> and Sebastiano Stramaglia<sup>1,2,3</sup>

<sup>1</sup>*TIRES-Center of Innovative Technologies for Signal Detection and Processing,  
Università di Bari, Italy*

<sup>2</sup>*Dipartimento Interateneo di Fisica, Bari, Italy*

<sup>3</sup>*Istituto Nazionale di Fisica Nucleare,  
Sezione di Bari, Italy*

(Dated: December 5, 2021)

We generalize a previously proposed approach for nonlinear Granger causality of time series, based on radial basis function. The proposed model is not constrained to be additive in variables from the two time series and can approximate any function of these variables, still being suitable to evaluate causality. Usefulness of this measure of causality is shown in a physiological example and in the study of the feed-back loop in a model of excitatory and inhibitory neurons.

PACS numbers: 05.10.-a, 87.10.+e, 87.19.La

## I. INTRODUCTION

Since the seminal paper by Granger [1], detecting causality relationships between two simultaneously recorded signals is one of the most important problems in time series analysis. Applications arise in many fields, like economy [2], brain studies [3, 4, 5, 6, 7, 8], human cardiorespiratory system [9], and many others. The major approach to this problem examines if the prediction of one series could be improved by incorporating information of the other, as proposed by Granger. In particular, if the prediction error of the first time series is reduced by including measurements from the second time series in the regression model, then the second time series is said to have a causal influence on the first time series. As Granger causality was originally developed for linear systems [1], recently some attempts to extend this concept to the nonlinear case have been proposed. In [10] local linear models in reduced neighborhoods are considered and the average causality index, over the whole data-set, is proposed as a nonlinear measure. In [11] a radial basis function (RBF) approach has been used to model data, while in [12] a non-parametric test of causality has been proposed, based on the concept of *transfer entropy*. A recent paper [13] pointed out that not all nonlinear prediction schemes are suitable to evaluate causality between two time series, since they should be invariant if statistically independent variables are added to the set of input variables. This property guarantees that, at least asymptotically, one would be able to recognize variables without causality relationship. The purpose of this work is to use the theoretical results found in [13] to find the largest class of RBF models suitable to evaluate causality, thus extending the results described in [11]. Moreover we show the application of causality to the analysis of cardiocirculatory interaction and to study the mutual influences in inhibitory and excitatory model neurons.

Let  $\{\bar{x}_i\}_{i=1,..,N}$  and  $\{\bar{y}_i\}_{i=1,..,N}$  be two time series of  $N$  simultaneously measured quantities. In the following we will assume that time series are stationary. We aim at quantifying *how much  $\bar{y}$  is cause of  $\bar{x}$* . For  $k = 1$  to  $M$  (where  $M = N - m$ ,  $m$  being the order of the model), we denote  $x^k = \bar{x}_{k+m}$ ,  $\mathbf{X}^k = (\bar{x}_{k+m-1}, \bar{x}_{k+m-2}, \dots, \bar{x}_k)$ ,  $\mathbf{Y}^k = (\bar{y}_{k+m-1}, \bar{y}_{k+m-2}, \dots, \bar{y}_k)$  and we treat these quantities as  $M$  realizations of the stochastic variables  $(x, \mathbf{X}, \mathbf{Y})$  [14]. Let us now consider the general nonlinear model

$$x = w_0 + \mathbf{w}_1 \cdot \Phi(\mathbf{X}) + \mathbf{w}_2 \cdot \Psi(\mathbf{Y}) + \mathbf{w}_3 \cdot \Xi(\mathbf{X}, \mathbf{Y}), \quad (1)$$

where  $w_0$  is the bias term,  $\{\mathbf{w}\}$  are real vectors of free parameters,  $\Phi = (\varphi_1, \dots, \varphi_{n_x})$  are  $n_x$  given nonlinear real functions of  $m$  variables,  $\Psi = (\psi_1, \dots, \psi_{n_y})$  are  $n_y$  other real functions of  $m$  variables, and  $\Xi = (\xi_1, \dots, \xi_{n_{xy}})$  are  $n_{xy}$  functions of  $2m$  variables. Parameters  $w_0$  and  $\{\mathbf{w}\}$  must be fixed to minimize the prediction error (we assume  $M \gg 1 + n_x + n_y + n_{xy}$ ):

$$\epsilon_{xy} = \frac{1}{M} \sum_{k=1}^M (x^k - w_0 - \mathbf{w}_1 \cdot \Phi(\mathbf{X}^k) - \mathbf{w}_2 \cdot \Psi(\mathbf{Y}^k) + \mathbf{w}_3 \cdot \Xi(\mathbf{X}^k, \mathbf{Y}^k))^2. \quad (2)$$

We also consider the model:

$$x = v_0 + \mathbf{v}_1 \cdot \Phi(\mathbf{X}), \quad (3)$$

and the corresponding prediction error  $\epsilon_x$ . If the prediction of  $\bar{x}$  improves by incorporating the past values of  $\{\bar{y}_i\}$ , i.e.  $\epsilon_{xy}$  is smaller than  $\epsilon_x$ , then  $y$  is said to have a causal influence on  $x$ . We must require that, if  $\mathbf{Y}$  is statistically

independent of  $x$  and  $\mathbf{X}$ , then  $\epsilon_{xy} = \epsilon_x$  at least for  $M \rightarrow \infty$ . This is ensured if, for each  $\alpha \in \{1, \dots, n_{xy}\}$ , an index  $i_\alpha$  exists such that:

$$\xi_\alpha(\mathbf{X}, \mathbf{Y}) = \varphi_{i_\alpha}(\mathbf{X})\Gamma_\alpha(\mathbf{Y}), \quad (4)$$

where  $\Gamma_\alpha$  is an arbitrary function of  $\mathbf{Y}$ . As explained in [13], model (1), with condition (4), is the largest class of nonlinear parametric models suitable to evaluate causality. We remark that  $\epsilon_{xy}$  is equal to  $\epsilon_x$  also at finite  $M$ , for statistically independent  $\mathbf{Y}$ , if the probability distribution is replaced by the empirical measure. Exchanging the two time series, one may analogously study the causal influence of  $x$  on  $y$ .

We choose the functions  $\Phi$ ,  $\Psi$  and  $\Xi$ , in model (1), in the frame of RBF methods thus generalizing the approach in [11]. We fix  $n_x = n_y = n_{xy} = n \ll M$ :  $n$  centers  $\{\tilde{\mathbf{X}}^\rho, \tilde{\mathbf{Y}}^\rho\}_{\rho=1}^n$ , in the space of  $(\mathbf{X}, \mathbf{Y})$  vectors, are determined by a clustering procedure applied to data  $\{(\mathbf{X}^k, \mathbf{Y}^k)\}_{k=1}^M$  (we use fuzzy c-means [15] to find prototypes). We then make the following choice for  $\rho = 1, \dots, n$ :

$$\begin{aligned} \varphi_\rho(\mathbf{X}) &= \exp\left(-\|\mathbf{X} - \tilde{\mathbf{X}}^\rho\|^2/2\sigma^2\right), \\ \psi_\rho(\mathbf{Y}) &= \exp\left(-\|\mathbf{Y} - \tilde{\mathbf{Y}}^\rho\|^2/2\sigma^2\right), \\ \xi_\rho(\mathbf{X}, \mathbf{Y}) &= \varphi_\rho(\mathbf{X})\psi_\rho(\mathbf{Y}), \end{aligned} \quad (5)$$

$\sigma$  being a fixed parameter, whose order of magnitude is the average spacing between the centers. Condition (4) is satisfied by construction. The RBF model of [11] is recovered setting  $\Xi = \mathbf{0}$  in (1), i.e. it is constrained to be additive in variables  $\mathbf{X}$  and  $\mathbf{Y}$ ; instead the RBF model, here proposed, can approximate any function of  $\mathbf{X}$  and  $\mathbf{Y}$ .

Now we describe the application to time series of heart rate and blood pressure from patients from an intensive care unit, contained in the MIMIC database [16]. In healthy subjects the heart rate variability (HRV) and the systolic blood pressure (SBP) are interdependent. Two mechanisms determine the feed-forward influence of HRV on SBP, the Starling law and the diastolic decay; baroreflex regulation determines the influence of SBP on HRV [17]. We consider signals from six patients affected by congestive heart failure (CHF)/pulmonary edema (patients no. 212, 213, 214, 225, 230, and 245) and six patients whose primary pathology was sepsis, a condition in which the body is fighting a severe infection and that can lead to shock, a reaction caused by lack of blood flow in the body (patients no. 222, 224, 269, 291, 410, and 422). HRV and SBP time series are extracted from raw data and re-sampled at  $2Hz$ . We fix  $n = 20$  and vary  $m$  from 1 to 20, taking  $\sigma = 2.5/\sqrt{m}$ . Denoting  $x$  the HRV time series, and  $y$  the SBP time series, figure 1 shows the behavior of  $\epsilon_x$  and  $\epsilon_y$  as a function of  $m$  for a typical subject. The optimal value of  $m$  corresponds to the knee of the curves,  $m = 5$ : in terms of frequency this value corresponds to the respiratory band. In figure 2 we depict  $\delta_1 = (\epsilon_x - \epsilon_{xy})/\epsilon_x$  (measuring the influence of SBP on HRV) and  $\delta_2 = (\epsilon_y - \epsilon_{yx})/\epsilon_y$  (measuring the influence of HRV on SBP), as a function of  $m$ , for CHF and sepsis patients. In the case of sepsis patients, the curves show a symmetric HRV-SBP interdependence, whilst in CHF patients the  $HRV \rightarrow SBP$  influence seems to be dominant, as  $\delta_2$  shows a peak at  $m = 5$ . The probability that the twelve  $\delta_2$  values, from all subjects and corresponding to  $m = 5$ , were drawn from the same population has been estimated by Wilcoxon test to be less than  $10^{-2}$ . The average directionality index  $D$  [11], at  $m = 5$ , is equal to 0.82 for CHF patients and to  $-0.019$  for sepsis patients. These results show, on one side, that sepsis condition is not characterized by unbalanced HRV-SBP loop interaction. On the other hand, it is well known that CHF patients show unbalanced HRV-SBP regulatory mechanism, the feed-forward HRV $\rightarrow$ SBP coupling being prevalent over baroreflex sensitivity [18]: our findings show that this effect may be described in terms of Granger causality between HRV and SBP time series.

As a second application, we consider the interactions in a model of inhibitory and excitatory neurons, which has been studied from different points of view, and with different aims. Much attention have been dedicated to the mechanisms underlying modulation of visual processing by means of attention [19]. Synchronization originating from feedback can be one way to explain this process of selective attention. In a previous study [20], it has been shown that inhibitory feedback is a way for the neurons to distinguish between spatially correlated and uncorrelated input. So it is important to study causal influences in a closed feedback-feedforward loop, and to understand how the inhibitory feedback, responsible of the selectivity of the attention, modifies the causal relationships between the neurons in the excitatory population. Here we consider the following question: what does causality measure in the case of coupled firing neurons? We show that it does not merely measure coupling constants, but the combined influence of couplings and membrane time constants. We consider a model of interacting neurons, two excitatory and one inhibitory, as illustrated in figure 3. This is a simplified case of the models in [20], [21] and [22]. All neurons are Leaky Integrate-and-Fire (LIF) neurons with a membrane potential  $V$  and an input current  $I$  satisfying:

$$\dot{V} = -V + I, \quad (6)$$

where time is measured in units of the membrane time constant and the membrane resistance is set to one. We denote  $\tau_E$  ( $\tau_I$ ) the membrane time constant of excitatory (inhibitory) neurons. Every time the potential of a neuron reaches

the threshold value  $V_{th}$ , a spike is fired. This resets the potential to the value  $V_R$ ; it remains bound to this value for an absolute refractory period  $\tau_R$ . Furthermore we normalize the reset value  $V_R$  to zero and the threshold value  $V_{th}$  to one. The series of spikes  $S_j^E(t)$  ( $j = 1, 2$ ) from excitatory neurons provide the input current  $I_I$  to the inhibitory LIF neuron, given by the convolution of the sum of the spike trains of the excitatory neurons and a standard  $\alpha$  function, which mimics an excitatory post-synaptic potential (EPSP). As a consequence of the excitatory input, the inhibitory neuron fires action potentials. As in the case of the excitatory current, the action potential  $S^I(t)$  of the inhibitory neuron provides the input currents  $I_{E,j}$  to the excitatory neurons by convolution of the spike train from the inhibitory neuron and an inhibitory post-synaptic potential (IPSP), given by the same  $\alpha$  function used to represent the EPSP, but reversed in sign. This inhibitory feedback is characterized by a gain  $g$ , and it's delivered after a delay time  $\tau_D$ . Summarizing, for each excitatory neuron  $j = 1, 2$  the total input current  $I_{E,j}$  is given by

$$I_{E,j}(t) = \mu + \eta_j(t) - g \int_0^\infty d\tau s^I(t - \tau - \tau_D) \alpha^2 \tau e^{-\alpha\tau}, \quad (7)$$

while the input current for the inhibitory neuron is

$$I_I(t) = \mu + \int_0^\infty d\tau (S_1^E(t - \tau) + S_2^E(t - \tau)) \alpha^2 \tau e^{-\alpha\tau}, \quad (8)$$

where  $\mu$  is a constant base current and  $\eta_j(t)$  represents internal Gaussian white noise with intensity  $K$ . We use  $\mu = 0.5$ ,  $K = 0.08$ ,  $\alpha = 18$  ms and  $\tau_D = 18$  ms.  $\tau_R$  is set to 3 ms, while  $\tau_E = \tau_I = 6$  ms. Note that the base current is below threshold, therefore the inhibitory neuron only fires in response to excitatory spike input. Moreover, using these parameters, the feedback model is a very stable one, resulting in firing rates from all neurons being almost independent on the values of membrane time constants and inhibitory feedback gain  $g$  used in this study. The firing rates of all the three neurons are always between 40 and 60 Hz. The model equations have been numerically solved by Euler integration using a time step 0.1 ms. The causal relationships between the time series of membrane potentials from neurons are then evaluated using the proposed RBF approach with  $n = 20$  and  $\sigma = 2.5/\sqrt{m}$ ,  $m \in [1, 600]$ . In absence of inhibitory feedback, i.e.  $g = 0$ , there is a dominant causal influence of the excitatory input on the inhibitory one; on the other hand, when the feedback is turned on ( $g = 1.2$ ), the causal influence is reversed, see figure 4. It is worth stressing, however, that in this context the measure of causality is not simply related to coupling  $g$ . Indeed, if we consider the same situation, but with a longer membrane time constant of the inhibitory neuron  $\tau_I$ , the influence of the latter on the excitatory ones is notably reduced (see figure 4). This can be explained in the following way. When the time constant is short, the inhibitory neuron behaves as a coincidence detector and inhibitory feedback has the effect of synchronizing the excitatory neurons [22], which thus tend to fire at the same time. For longer membrane time constant, the inhibitory neuron acts as an integrator and does not discriminate between two temporally close spikes; the inhibitory neuron then reacts to a smaller number of input spikes, resulting in a decreased causal influence on the two excitatory neurons.

Another interesting situation corresponds to only one, out of the two, excitatory neuron receiving inhibitory feedback: we then investigate the causal relationships between the two excitatory neurons, as mediated by the inhibitory one. In absence of inhibitory feedback there is no causality involved. As the feedback is switched on, as it is clear in figure 5, a significant causal influence, of the neuron which does not receive the feedback on the other, is observed. Even in this case, the causal influence depends also on the membrane time constant of the inhibitory neuron, which may act as a coincidence detector or as an integrator, thus considering two successive spikes from the two excitatory neurons as two separates spikes, or as one, respectively. This mechanism of selective feedback can be used to explain the phenomenon of stimulus recognition with biased attention in the visual cortex [19].

We have generalized the RBF approach to Granger causality so that any function of the input variables can be approximated. The two applications here considered show the usefulness of the proposed approach and, more generally, of the notion of causality.

**Acknowledgements.** Valuable discussions with Nicola Ancona and Stan Gielen are warmly acknowledged.

- 
- [1] C.W.J. Granger, *Econometrica* **37**, 424 (1969).
  - [2] J.J. Ting, *Physica A* **324**, 285 (2003).
  - [3] P. Tass et al., *Phys. Rev. Lett.* **81**, 3291 (1998); M. Le van Quyen et al., *Brain Res.* **792**, 24 (1998).
  - [4] S. J. Schiff et al., *Phys. Rev. E* **56**, 6708 (1996); M. Wiesenfeldt, U. Parlitz, W. Lauterborn, *Int. Jour. of Bifurcation and Chaos* **11**, 2217 (2001).
  - [5] R. Sowa et al., *Phys. Rev. E* **71**, 61926 (2005).

- [6] K.J. Blinowska, R. Kus and M. Kaminski, Phys. Rev. E **70**, 50902(R) (2004).
- [7] M. G. Rosenblum et al., Phys. Rev. E **64**, 45202R (2001); M. Palus, A. Stefanovska, Phys. Rev. E **67**, 55201R (2003).
- [8] E. Pereda, R. Quiñan Quiroga, J. Bhattacharya, Progress in Neurobiology **77** 1 (2005).
- [9] M. G. Rosenblum et al., Phys. Rev. E **65**, 41909 (2002).
- [10] Y. Chen et al., Phys. Lett. A **324**, 26 (2004).
- [11] N. Ancona, D. Marinazzo and S. Stramaglia, Phys. Rev. E **70**, 56221 (2004).
- [12] P.F. Verdes, Phys. Rev. E **72**, 26222 (2005).
- [13] N. Ancona and S. Stramaglia, cond-mat/0502511 (in press in Neural Computation).
- [14] Usually both times series are normalized in the preprocessing stage, i.e. they are linearly transformed to have zero mean and unit variance.
- [15] J. C. Bezdek, *Pattern Recognition with Fuzzy Objective Function Algorithms* (Plenum Press, New York, 1981).
- [16] <http://www.physionet.org/>
- [17] *Mechanisms of blood pressure waves*, K. Miyakawa, C. Polosa, H.P. Koepchen (eds.). Springer, Berlin Heidelberg New York (1984).
- [18] G.D. Pinna et al., J. Am. Coll. Cardiol. **46**, 1314 (2005).
- [19] J.R. Reynolds et al., J. Neurosci. **19**, 1736 (1999).
- [20] B. Doiron et al., Phys. Rev. Lett. **93**(4), 048101 (2004).
- [21] D. Marinazzo, H.J. Kappen, S. Gielen, *Input-driven oscillations in networks with excitatory and inhibitory neurons with dynamic synapses*, submitted.
- [22] C. Börgers and N. Kopell, Neural Computation **15**, 509 (2003).

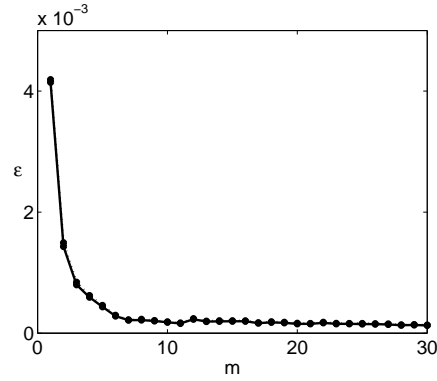


FIG. 1:  $\epsilon_x$  and  $\epsilon_y$  (indistinguishable) are plotted vs  $m$ , for a typical patient.

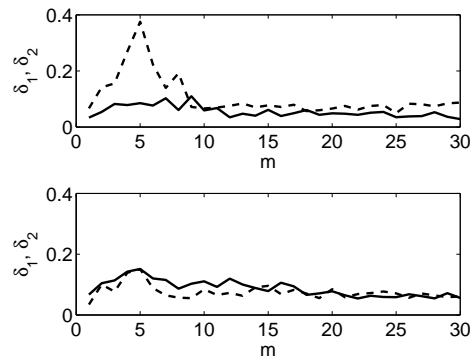


FIG. 2:  $\delta_1$  (full line) and  $\delta_2$  (dashed line) are plotted vs  $m$ , averaged over CHF patients (above), and averaged over sepsis patients (below).

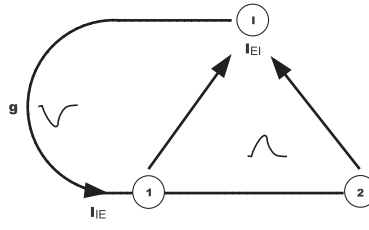
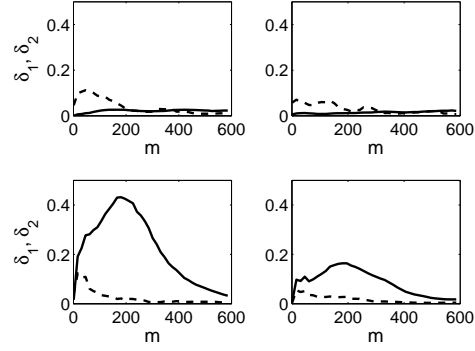
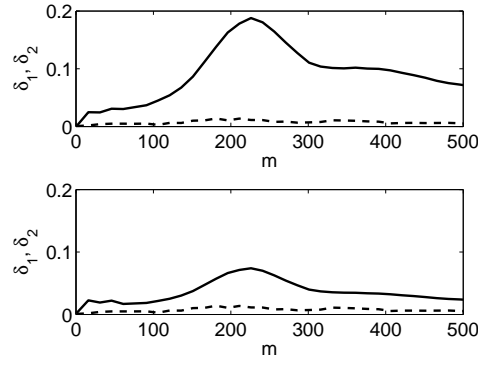


FIG. 3: Neural model architecture.

FIG. 4:  $\delta_1$  (full line,  $I \rightarrow E$ ) and  $\delta_2$  (dashed line,  $E \rightarrow I$ ) are plotted vs  $m$ , for  $\tau_I = \tau_E = 6ms$  (left), and  $\tau_I = 18ms$ ,  $\tau_E = 6ms$  (right). Above, no feedback. Below, with feedback.FIG. 5:  $\delta_1$  (full line, influence of the excitatory neuron without feedback on the one with feedback) and  $\delta_2$  (dashed line, influence of the excitatory neuron with feedback on the one without feedback) are plotted vs  $m$ , for  $g = 1.2$ .  $\tau_I = \tau_E = 6ms$  (top);  $\tau_I = 18ms$ ,  $\tau_E = 6ms$  (bottom).